Effect of Homogenization Heat Treatment on the Microstructure and Heat-Affected Zone Microfissuring in Welded Cast Alloy 718

XIAO HUANG, M.C. CHATURVEDI, and N.L. RICHARDS

The effect of homogenization temperature on microfissuring in the heat-affected zones of electron-beam welded cast INCONEL 718 has been studied. The material was homogenized at various temperatures in the range of 1037 °C to 1163 °C and air-cooled. The homogenized material was then electron-beam welded by the bead-on-plate welding technique. The microstructures and microfissuring in the heat-affected zone (HAZ) were evaluated by analytical scanning electron microscopy (SEM). The grain boundary segregation of various elements was evaluated by secondary ion mass spectroscopy (SIMS). It was observed that the total crack length (TCL) of microfissures first decreases with homogenization temperature and then increases, with a minimum occurring in the specimen heat treated at 1163 °C. This trend coincides with the variation in segregation of B at grain boundaries with homogenization temperature and has been explained by equilibrium and nonequilibrium segregation of B to grain boundaries during the homogenization heat treatment. No other element was observed to segregate at the grain boundaries. The variation in volume fraction of phases like δ-Ni_3Nb, MC carbide, and Laves phases does not follow the same trend as that observed for TCL and B segregation at the grain boundaries. Therefore, microfissuring in HAZ of welded cast INCONEL 718 is attributed to the segregation of B at the grain boundaries.

I. INTRODUCTION

INCONEL* 718 is a γ''-precipitation-hardened Ni-Fe-Cr base alloy that was developed for aerospace applications in the 1960s.[1] The presence of Nb in this alloy makes it free from strain-age cracking; however, it promotes intergranular and interdendritic cracking in the fusion and heat-affected zones (HAZs) in welded regions.

The alloy was originally utilized in wrought form, and most of the welding research reported in the literature was conducted on wrought alloy. It was found that HAZ microfissuring in this condition can be controlled through reducing the grain size.[2] Recently, an increasing number of large components, such as compressors and turbine frames, are being made of cast alloy 718, they require a reduced amount of machining and welding.[3] Compared to wrought alloy 718, more severe microfissuring has been observed in cast alloy 718, which could be attributed to the coarse grain size and greater presence of a low-melting-point Laves phase as a result of heavy dendritic segregation.

The effect of heat treatment prior to welding has been examined by several investigators;[4–8] however, no systematic study has been conducted in the past. This article describes the results of an investigation on the influence of heat treatment on the microstructure and HAZ microfissuring of cast alloy 718. Heat-affected-zone microfissuring has been discussed in terms of the volume fraction of second phases, grain boundary precipitates, hardness, and grain boundary elemental segregation.

*INCONEL is a trademark of Inco Alloys International, Inc., Huntington, WV.

XIAO HUANG, Material & Processes Engineer, is with Bristol Aerospace Ltd., and M.C. CHATURVEDI, Professor, is with the Department of Mechanical Engineering, University of Manitoba, Winnipeg, MB, Canada R3T 2N2. N.L. RICHARDS, Manager, Material & Processes/Facilities Engineering, is with Bristol Aerospace Ltd., Winnipeg, MB, Canada.

Manuscript submitted September 3, 1993.

II. EXPERIMENTAL TECHNIQUES

The as-received material was alloy 718 plates (1.6 × 5 × 15 cm) produced by investment casting at P.C.C. (Portland, OR). The chemical composition of the as-received material is given in Table I. The plates were sectioned into 1.6 × 5 × 5-cm test specimens and were given various preweld heat treatments in an air furnace within the temperature range of 1037 °C to 1163 °C (summarized in Table II). The heat-treated specimens were gas tungsten arc spot welded onto a large plate to establish restraint and then were welded by the bead-on-plate technique by a Sciaky Mark VII electron-beam welder using a sharp focus (without beam oscillation) at 44 kV, 79 mA, and 152 cm/min. A partial penetration weld was achieved.

The microstructure of the base material was examined by scanning electron microscopy (SEM) using the secondary and backscattered electron image modes. Phases were identified by their morphologies and chemical compositions. A JEOL* 840 scanning electron microscope equipped with a NORAN energy-dispersive spectroscopy (EDS) system with a NORVAR detector window enabled a qualitative analysis of light elements such as C and N. Volume fractions of microstructural constituents were measured using a LEITZ** Image Analyzer, 4000 points being counted for

*JEOL is a trademark of Japan Electron Optics Ltd., Tokyo, Japan.

**LEITZ is a trademark of E. Leitz, Inc., Rockleigh, NJ.

Table I. Chemical Composition of Cast Alloy 718 (Weight Percent)

C*	Mn	Si	Cr	Ni	Mo	Co
0.07	0.03	0.16	18.61	52.97	3.06	0.09
Nb	Al	Ti	P*	B*	S*	Fe
5.01	0.45	0.81	0.009	0.003	0.005	balance

*Analyzed from cast alloy sample. Other elements were from mill master heat compositions.

Table II. Heat Treatment Parameters

Number	1	2	3	4	5
Heat treatment	Cast	1037 °C/1h	1066 °C/1h	1093 °C/1h	1163 °C/1h
Cooling	—	A.C.*	A.C.	A.C.	A.C.& W.Q.**

W.Q. = water-quenched.
A.C. = air-cooled.
*20 °C/s (measured by implanted calibrated thermocouple in the center of specimen).
**400 °C/s.

each phase, with the standard deviation of the measurement indicated in Figure 3.

The welded specimens were cut into sections perpendicular to the welding direction. The microfissuring tendency after different heat treatments was evaluated using total crack length (TCL') measurements:

$$TCL' = \Sigma\, l_1 + l_2 + l_3 + \ldots$$

where l_1, l_2, and l_3 are individual crack length measurements from one section. To statistically increase the reliability of the *TCL'* value, measurements were made on 12 sections from one weldment for each heat treatment, and the sum of these values was used as the TCL in this investigation, *i.e.*,

$$TCL = \sum_{n=1}^{12} [TCL'_1, + TCL'_2, + TCL'_3, + ... + TCL'_{12}]$$

The average of TCL and its standard deviation were also calculated and used as comparison with the TCL in this study. Crack length measurements were made on a scanning electron microscope at a magnification of 550 times and 39-mm working distance.

Grain boundary elemental segregation was studied by secondary ion mass spectrometry (SIMS). The instrument used for SIMS analysis was a Cameca IMS-4f ion microscope using 14.5-KeV O_2^+ as the primary ion source. The negatively charged secondary ions emitted from the surface were used to obtain mass-resolved ion images. The samples for SIMS analysis were mechanically polished and electrolytically etched in 10 pct oxalic acid. Microhardness indentations were employed to locate the grain boundary in the etched condition, and the samples were then repolished to remove the etched surface layer.

III. RESULTS AND DISCUSSION

The as-cast alloy was severely segregated, as seen in the backscattered electron SEM image illustrated in Figure 1, with the lighter regions being the interdendritic area. The

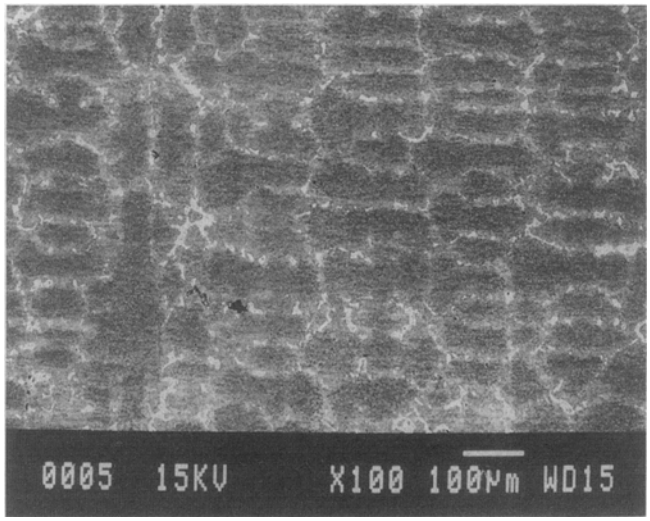

Fig. 1—Backscattered electron SEM image of dendritic structure of as-cast INCONEL 718.

secondary electron SEM image of as-cast structure is shown in Figure 2. The microstructure of the as-cast alloy consisted of γ matrix, cubic Ti(C,N) (Figure 2(a)) irregular-shaped Nb(C,N) (Figure 2(a)), lamellar (eutecticlike) Laves phase, and needlelike δ-Ni_3Nb (Figure 2(b)). The nonmatrix phases were present mainly in the interdendritic area; however, some carbides (or carbonitrides) were also observed in the dendrite core area. The alloy used in this study has a grain size ranging from 2 to 10 mm, which was not affected by the heat treatments. The microstructure variation from plate to plate was not noticeable because all the plates were from the same heat and cast into the same size plates.

After the 1037 °C/1 h heat treatment, the microstructure had features similar to those observed in the as-cast condition, *i.e.*, γ-matrix, M(C,N), and Laves phase, but a smaller amount of δ-Ni_3Nb phase. The microstructural examination after the 1163 °C/1 h heat treatment, however, indicated that the δ-Ni_3Nb had completely dissolved and Laves phase was barely detectable, but the amounts of M(C,N) did not change during this heat treatment.

The volume fractions of various phases were measured after heat treatment and plotted against the heat treatment temperature in Figure 3. These quantitative values confirm the trends observed by the microstructural examination; the δ-Ni_3Nb phase goes into solid solution at about 1093 °C, and the majority of the Laves phase (95 pct) is in solid solution at 1163 °C. Carbides and carbonitrides were observed to be unaffected by the heat treatments.

The chemical compositions of various constituents were determined semiquantitatively by EDS, and the results are listed in Table III. A strong nitrogen peak was observed on the EDS spectrum of cubic-shaped M(N); however, the software was not able to quantify the percentage of nitrogen. Carbon was not detected in particles of this phase, and the phase was therefore identified as a Ti-rich nitride. Both carbon and nitrogen peaks were observed on the EDS spectrum of irregular-shaped M(C,N) particles; thus, they can be identified as carbonitrides.

Electron-beam bead-on-plate welding produced a nail-shaped weld with most of the HAZ microfissuring observed to have occurred on grain boundaries under the nail head.

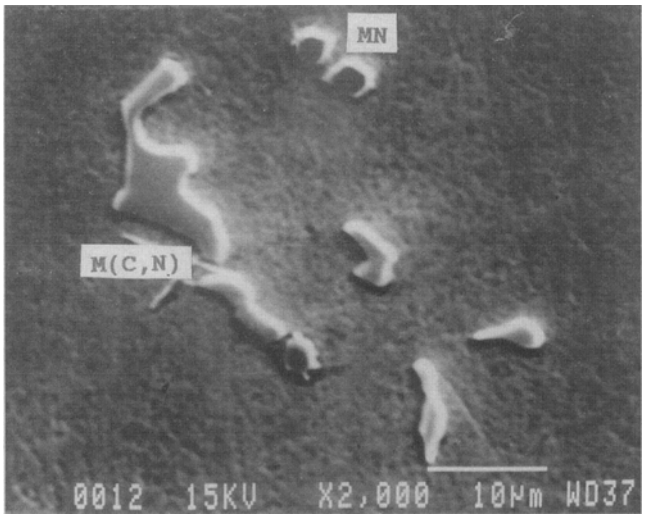

(*a*)

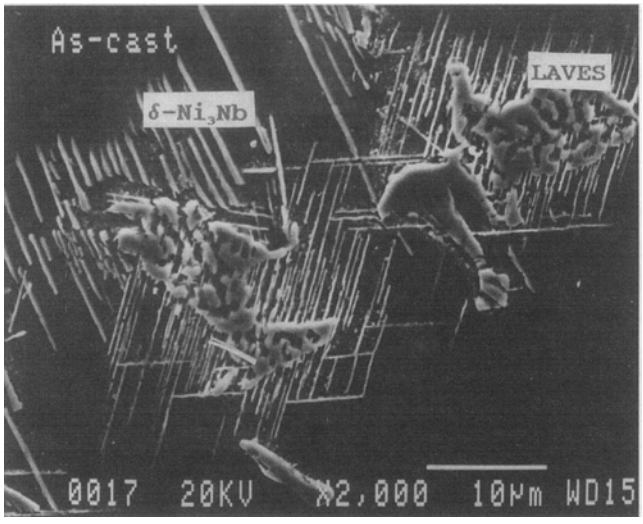

(*b*)

Fig. 2—Secondary electron SEM microstructure of INCONEL 718 in the as-cast condition containing (*a*) cubic Ti(C,N) and irregular-shaped Nb(C,N) and (*b*) lamellar Laves phase and needle-shaped δ-Ni_3Nb.

An example of this is shown in Figure 4. The values of TCL were measured, and a plot of these values against the heat treatment temperature is shown in Figure 5(a). The TCL value of the as-cast specimen is also shown in Figure 5(a) for comparison. The standard deviation at 90 pct confidence level for the average crack length was calculated, and the error bars were placed on the average crack length *vs* heat treatment temperature curve (Figure 5(b)). Similar trends were observed in both TCL and average crack length.

The influence of heat treatment temperature on microfissuring in alloy 718 has been examined by several investigators. In the wrought alloy, it has been shown that a high-temperature homogenization heat treatment increases microfissuring when grain size is maintained constant.[4,5,6] Thompson *et al.*[7] obtained approximately 9 to 12 pct increase in TCL after 1093 °C/1 h treatment over that observed in the as-cast condition. Kelly[8] has reported a 31 pct increase in TCL on changing the heat treatment from

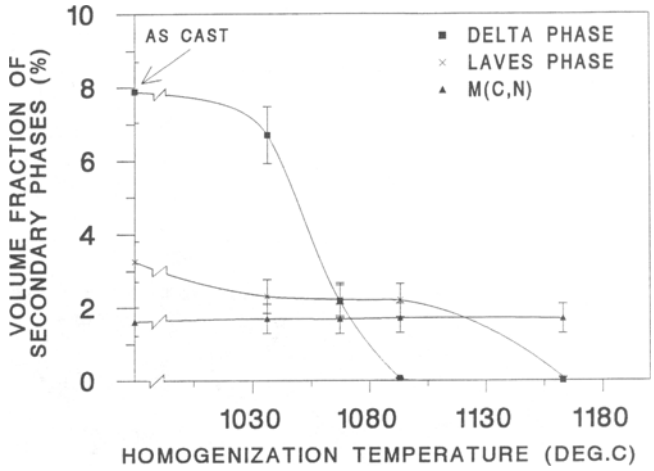

Fig. 3—Variations in volume fraction of Laves, δ-Ni_3Nb, and M(C,N) phases with heat treatment temperatures.

1093 °C/1 h to 1163 °C/1 h + 1093 °C/1 h. However, the present study showed that high-temperature homogenization heat treatment in the range of 1037 °C to 1066 °C decreases the TCL as compared with that observed in the as-cast condition, and the TCL value increases when the homogenization treatment is within the temperature range of 1066 °C to 1163 °C (Figure 5). It is also observed from Figure 3 that as the heat treatment temperature is increased, the amount of Laves phase decreases and the volume fraction of MC carbides remains constant, but the TCL-temperature curve does not follow the general trend of change in the volume traction of secondary phases caused by the solution heat treatment. This suggests that there is a sufficient fraction of liquid produced during the welding cycle, regardless of the volume fraction of a particular type of secondary phase. In addition, hardness was not influenced[10] by the various heat treatments used in this study, suggesting that hardness did not cause the observed variation in the values of TCL.

Kelly[8] has suggested the possibility of formation of a grain boundary film of resolidified Laves phase after homogenization at 1163 °C, which could increase the microfissuring. Transmission electron microscopy (TEM) in the present work, however, failed to reveal any precipitate film on the grain boundaries.

Thompson *et al.*[9] concluded that tramp elements (such as S) can be released during heat treatment and can segregate to grain boundaries. Their investigation by Auger spectroscopy showed segregation of S to free surfaces and grain boundaries after a 1093 °C homogenization treatment; however, sulfur segregation to the grain boundaries was not observed through SIMS analysis by the present authors.[10]

Boron has been considered to influence microfissuring by affecting the wetting behavior of liquid formed on grain boundaries.[8] It was suggested that B is the main element contributing to microfissuring that could be attributed to the decomposition of boride during heat treatment, although borides have not been observed in cast alloy 718 by the present authors. Another possible explanation is that during homogenization heat treatment, B (from solid solution) segregation to grain boundaries may occur to reduce the free energy of the system. However, this equilibrium segregation theory[11] leads one to conclude that increasing tem-

Table III. Chemical Composition of Various Phases Determined by EDS

	(Weight Percent)							
	Fe	Ni	Cr	Mo	Nb	Ti	Al	Si
δ-Ni_3Nb	14.72	52.0	16.27	4.50	10.13	1.31	0.64	0.47
Laves	12.69	42.65	15.01	6.8	20.51	1.18	0.45	0.69
Nb-rich M(C,N)	0.53	1.74	0.93	4.28	86.62	5.91	0	0
Ti-rich M(N)	0.67	1.10	0.57	1.35	33.80	61.67	0.85	0

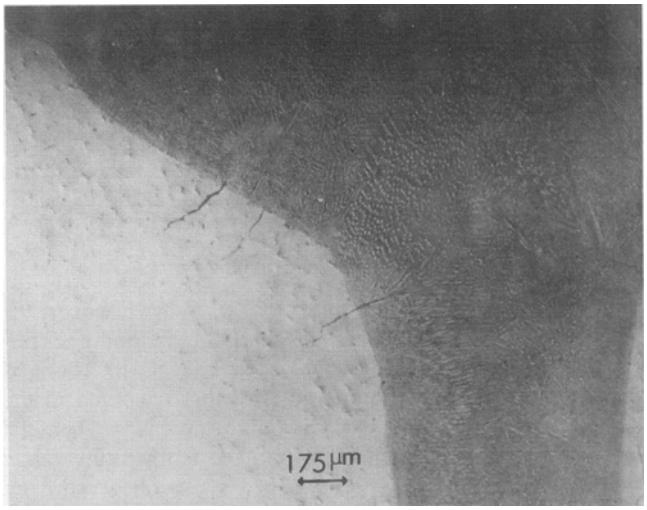

Fig. 4—HAZ microfissures under the nail head of an electron-beam weldment.

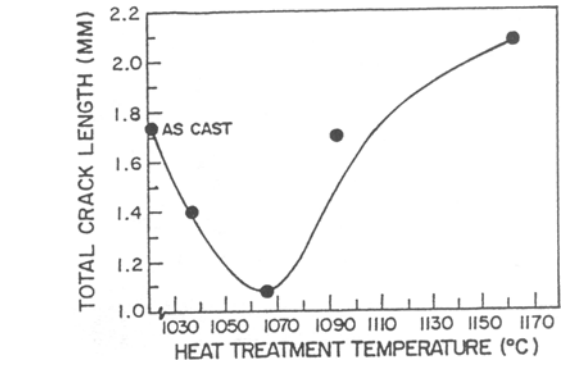

(*a*)

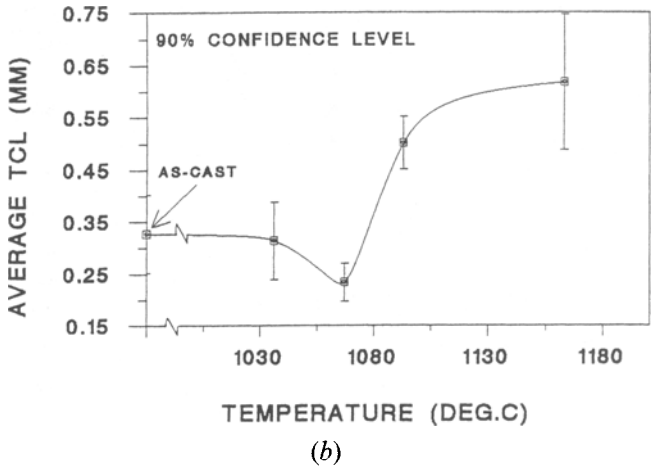

(*b*)

Fig. 5—(*a*) Variation of TCL and (*b*) average crack length in HAZ with heat treatment temperatures.

perature causes an increased solubility of elements in the matrix, resulting in reduced grain boundary segregation. The existing theories of HAZ microfissuring, *i.e.*, sulfur segregation to grain boundary, boride decomposition, and conventional equilibrium segregation theory, did not seem to be able to explain the observed variation in TCL with the heat treatment temperature shown in Figure 5. Additionally, neither the volume fraction of secondary phases nor the hardness values show any correlation with the variation in TCL. A reasonable interpretation can be provided, however, by the following hypothesis, which combines equilibrium and nonequilibrium segregation of boron in material heat-treated at different temperatures.

Equilibrium grain boundary segregation occurs when an alloy is held at a temperature sufficiently high to allow appreciable diffusion of impurities to the grain boundaries and thus reduce the free energy of the system, and the amount of equilibrium segregation decreases as the heat treatment temperature increases.[11] Nonequilibrium segregation occurs during cooling from high temperature, which was first proposed by Westbrook and Aust[12] and Anthony.[13] The mechanism of nonequilibrium segregation involves the formation of sufficient quantities of vacancy-impurity complexes. When the material is cooled through a large temperature range, the equilibrium concentration of vacancies (and thus complexes) is reduced. This equilibrium concentration cannot be achieved during intermediate cooling rate except at vacancy sinks such as grain boundaries. Thus, vacancy concentration gradients are formed, and there is a net flow of vacancies toward the vacancy sinks. The vacancy-impurity complexes are also carried down these gradients, and impurity atoms are deposited at vacancy sinks such as grain boundaries and interfaces. The amount of nonequilibrium segregation increases as heat treatment temperature increases, provided that the right combination of cooling rate, impurity complex coupling, and diffusivity occurs.[14] In addition to the equilibrium and nonequilibrium segregation of boron, the presence of boron in localized areas in the initial casting (as was occasionally observed in the non-heat-treated material) may also contribute to its overall concentration at the grain boundaries through the migration of B to the grain boundaries and to the matrix/secondary phase interfaces. The migration of B increases as the heat treatment temperature increases. The combined influence of the three effects can be represented by a summation of the three curves, as shown in a schematic form in Figure 6. The overall effect of these three factors on the segregation of B at the grain boundaries follows the same trend as the variation of the TCL with temperature shown in Figure 5. Therefore, in air-cooled material, as the heat treatment temperature is increased

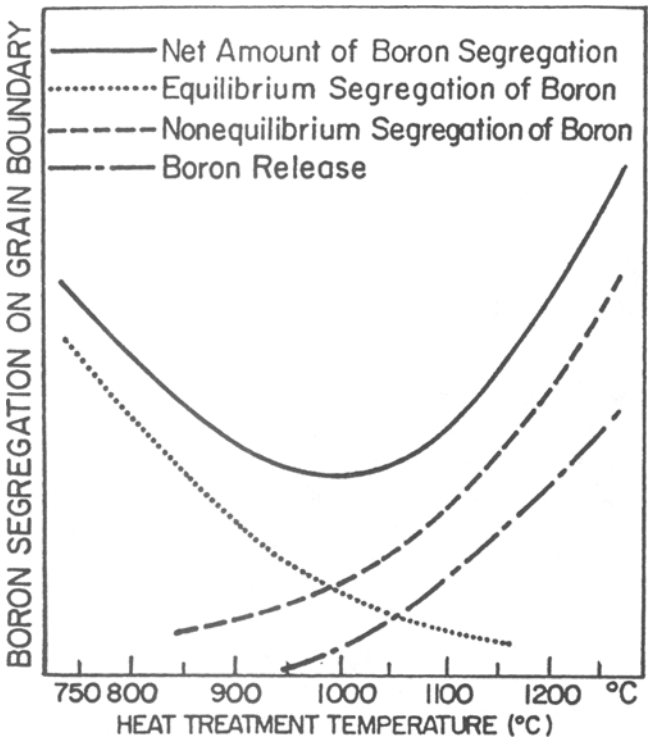

Fig. 6—Schematic diagram of boron segregation to the grain boundary as a result of equilibrium segregation, nonequilibrium segregation, and boron release from the boron concentrated areas after being heat-treated at different temperatures.[14]

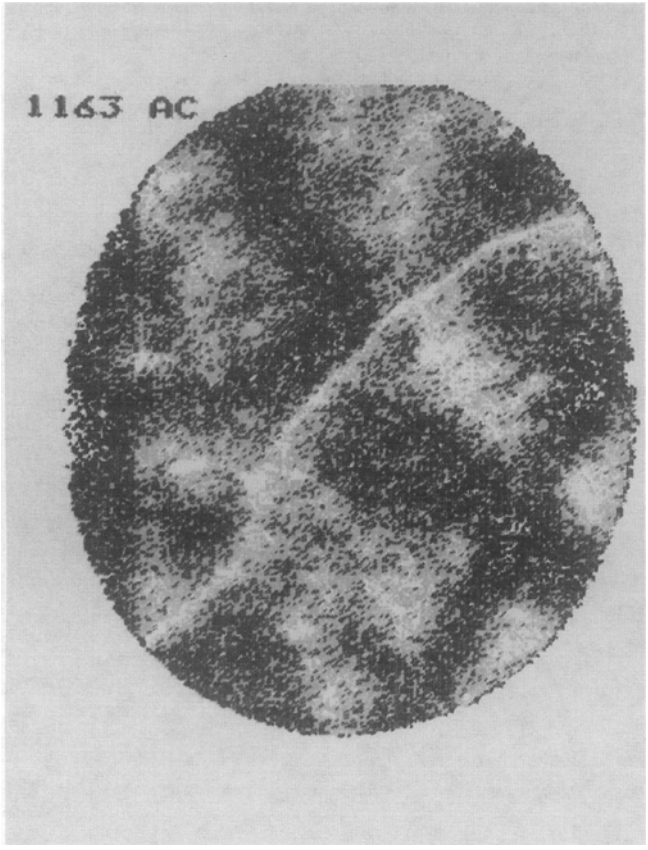

Fig. 7—SIMS micrograph showing boron segregation on grain boundaries after heat treatment at 1163 °C/h followed by air-cooling (magnification 250 times).

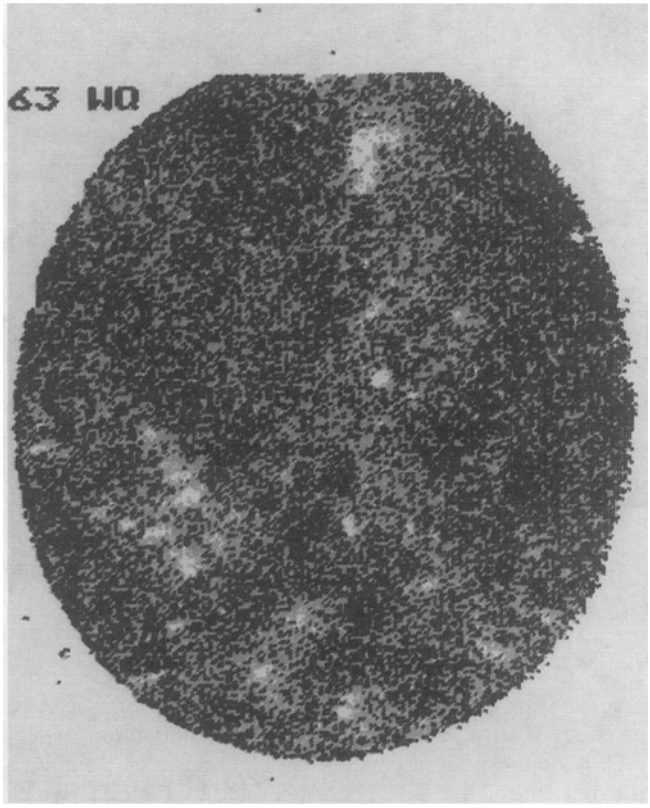

Fig. 8—SIMS micrograph showing boron distribution after heat treatment at 1163 °C/h followed by water-quench (magnification 250 times).

from 1037 °C, the segregation of boron decreases as a result of a decrease in equilibrium segregation. However, as the heat treatment temperature increases further, the nonequilibrium segregation of B becomes significant, and the segregation of B starts to increase. Therefore, it is suggested that the value of TCL first decreases and then increases with an increase in the heat treatment temperature because of a decrease in equilibrium segregation with temperature and an increase in B concentration with temperature.

To verify the proposed theory, a SIMS analysis was conducted to detect the existence of B on grain boundaries. The $^{10}B^{16}O_2^-$ signal on mass 42 is a unique channel on secondary ion spectrum. Although $^{11}B^{16}O_2^-$ signal recorded on mass 43 is the strongest boron channel, it overlaps with $^{27}Al^{16}O^-$, and because the cast alloy 718 contains Al, mass 42 is the best channel to collect the boron signal.

Preliminary SIMS analysis revealed that boron segregated to the grain boundaries after 1163 °C/1 h (a.c.) heat treatment (Figure 7). This specimen was observed to have the highest TCL. Water quenching after heat treatment (at 1163 °C) suppressed the occurrence of nonequilibrium segregation, as shown in Figure 8, indicating the existence of nonequilibrium boron segregation in the air-cooled specimen. Other elements, such as S, P, C, and Nb, were also examined; however, segregation of these elements to grain boundaries was not observed by SIMS analysis.[10] This seems to support the hypothesis that HAZ microfissuring in cast 718 may be due to the segregation of B at the grain boundaries. The effect of electron-beam welding thermal cycle on boron segregation was also considered. An implanted thermocouple showed that a peak temperature of

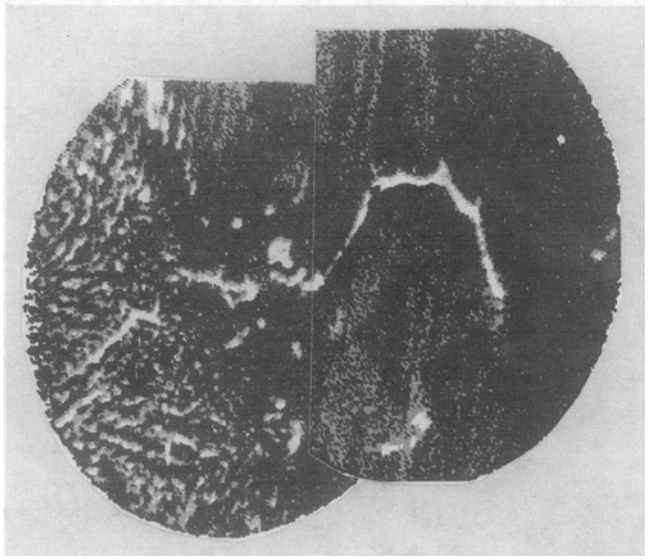

Fig. 9—SIMS micrograph showing boron distribution on HAZ microfissure (magnification 250 times).

1350 °C was reached in the HAZ in approximately 1 to 2 seconds. In 1 second, a boron atom would travel a distance of about 20 μm. The net effect is thus a reduction in segregation intensity as compared with that before welding, but it is not eliminated. This is corroborated by Figure 9, which shows boron segregation on HAZ crack.

Further work is being performed to study the boron segregation in specimens of this alloy heat-treated at various temperatures and cooled at different cooling rates (air-cool and water-quench) by SIMS.

IV. CONCLUSIONS

1. The microfissuring tendency in the HAZ of electron-beam-welded cast INCONEL 718 (as determined by TCL measurements) is observed to first increase and then decrease with an increase in homogenization temperature from 1037 °C to 1163 °C. The minimum value of TCL was observed in the specimen that was homogenized at 1066 °C.
2. The volume fraction of δ-Ni_3Nb and Laves phase was observed to decrease with an increase in homogenization temperature, but the volume fraction of MC carbide remained constant over the homogenization temperature range.
3. The SIMS analysis of elemental segregation at the grain boundaries revealed that B segregation first increases and then decreases with increasing homogenization temperature, and a minimum occurs in the specimen that was homogenized at 1066 °C, similar to TCL. No other element was observed to segregate at the grain boundaries. Therefore, the microfissuring in electron-beam-welded cast INCONEL 718 is attributed to the segregation of B at the grain boundaries.

ACKNOWLEDGMENTS

This work was financially supported by a grant from the University Industry Program of the Natural Sciences and Engineering Research Council of Canada, and by Bristol Aerospace Ltd., Winnipeg, MB, Canada. The assistance provided by Dr. J. Jackman of CANMET, Ottawa, in carrying out the SIMS analysis, is gratefully acknowledged.

REFERENCES

1. H.L. Eiselstein: in *Advances in the Technology of Stainless Steels and Related Alloys*, ASTM STP 369, Philadelphia, PA, 1965, pp. 62-77.
2. R.G. Thompson, J.J. Cassimus, D.E. Mayo, and J.R. Dobbs: *Welding J.*, 1985, vol. 66, pp. 91s-96s.
3. R.G. Carlson and J.F. Radavich: in *Superalloy 718—Metallurgy and Applications*, E.A. Loria, ed., Pittsburgh, PA, 1989, pp. 79-95.
4. R.G. Thompson and S. Genculu: *Welding J.*, 1983, vol. 62, pp. 337s-345s.
5. P.J. Valdez and J.B. Steinman: in *Effects of Minor Elements on the Weldability of High-Nickel Alloys*, Welding Research Council, New York, NY, 1969, pp. 93-120.
6. R.G. Thompson, J.R. Dobbs, and D.E. Mayo: *Welding J.*, 1986, vol. 65, pp. 299s-304s.
7. R.G. Thompson, D.E. Mayo, and B. Radhakrishnan: *Metall. Trans. A*, 1991, vol. 22A, pp. 557-67.
8. T.J. Kelly: *Welding J.*, 1989, vol. 70, pp. 44s-51s.
9. R.G. Thompson, B. Radhakrishnam, and D.E. Mayo: *J. Phys. Colloq.*, 1988, 49 (10), pp. 471-79.
10. X. Huang: Ph.D. Thesis, University of Manitoba, Winnipeg, MB, Canada, 1994.
11. M. Guttmann and D. Mclean: in *Interfacial Segregation*, W.C. Johnson and J.M. Balkely, eds., Metals Park, OH, 1979, pp. 261-347.
12. J.H. Westbrook and K.T. Aust: *Acta Metall.*, 1963, vol. 1, pp. 1151-63.
13. T.R. Anthony: *Acta Metall.*, 1969, vol. 17, pp. 603-09.
14. Xu Tingdong, Song Shenhua, Yuan Shexi, and Yu Zongsen: *J. Mater. Sci.*, 1990, vol. 25, pp. 1739-44.